Carbon 213 (2023) 118209

Contents lists available at ScienceDirect

Carbon

journal homepage: www.elsevier.com/locate/carbon

C_{60}+C_{60} molecular bonding revisited and expanded

Jorge Laranjeira [a,**], Karol Strutyński [b], Leonel Marques [a], Emilio Martínez-Núñez [c], Manuel Melle-Franco [b,*]

[a] Departamento de Física and CICECO, Universidade de Aveiro, 3810-193, Aveiro, Portugal
[b] Departamento de Química and CICECO, Universidade de Aveiro, 3810-193, Aveiro, Portugal
[c] Departamento de Química Física, Universidade de Santiago de Compostela, 15782, Santiago de Compostela, Spain

ARTICLE INFO

Keywords:
Fullerene dimers
DFT calculations
AutoMeKin
HOMO-LUMO Gap

ABSTRACT

Several dimerization products of fullerene C_{60} are presented and thoroughly characterized with a quantum chemical DFT model augmented by dispersion. We reanalyze and expand significantly the number of known dimers from 12 to 41. Many of the novel bonding schemes were found by analyzing more than 2 ns of high energy molecular dynamics semiempirical trajectories with AutoMeKin, a methodology previously used to compute the reactivity of much smaller molecules. For completeness, this was supplemented by structures built by different geometric considerations. Also, spin-polarization was explicitly considered yielding 12 new bonding schemes with magnetic ground states. The results are comprehensively analyzed and discussed in the context of yet to be explained 3D fullerene structures and recent fullerene 2D systems.

1. Introduction

At room temperature and atmospheric pressure, C_{60} is a van der Waals solid with a face-centered cubic (fcc) structure where the molecules are rotating freely [1]. When subjected to visible or ultraviolet light, or high-pressures high-temperatures (HPHT) treatments the C_{60} molecules bond to each other via 66/66 2+2 cycloaddition forming aggregates and dimers [2–4], see Fig. 1.

Increasing the pressure and temperature of the C_{60} HPHT treatment leads to the formation of extended crystalline networks [5–11]. At pressures below 8 GPa the formation of low-dimensionality polymers occurs yielding 1D orthorhombic, 2D tetragonal and 2D rhombohedral phases. In all these low-dimensionality polymers, the molecules arrange themselves in covalently bonded chains (1D) or sheets (2D) formed exclusively by 66/66 2+2 cycloadditions, Fig. 1.

It is above 8 GPa that fully 3D polymerized crystals are formed [8–11]. Here other bonding schemes, besides the 66/66 2+2 cycloaddition, start to play an important role, in fact, 3D polymers proposed to date have different bonding schemes such as the 56/56 2+2 cycloaddition [7,8], the 6/6 3+3 cycloaddition and the double 66/66 4+4 cycloaddition [9], the 56/65 2+2 cycloaddition and the 5/5 3+3 cycloaddition [10] or even the double 5/5 2+3 cycloaddition [11].

Recently, other C_{60} polymers have been produced from a different route [12,13]. This has yielded a pure carbon bulk material based on covalently linked fullerenes forming 2D sheets with hexagonal symmetry dubbed graphullerene [13]. These layers are bonded via single-bond and 56/65 2+2 cycloaddition, unlike any 2D polymers synthesized to date by HPHT treatment, showcasing the potential of alternative synthetic routes to produce new structures.

3D C_{60} polymers show quite remarkable physical properties for pure carbon phases, such as metallicity and low-compressibility which fosters interest in these materials [8–11]. Nevertheless, diffraction patterns from these phases lack the resolution needed to solve their crystalline structure. Thus, it is necessary to build complementary computational models fitting the overall symmetry and lattice parameters to the diffraction pattern and study their stability recurring to quantum simulation tools like Density Functional Theory (DFT) [7].

The distances between the two C_{60} covalently bonded molecules, i.e. a C_{60} dimer, computed from their molecular centers, Fig. 1, are similar to the corresponding distance in a bulk crystalline phase. For instance, the C_{60} molecular distance, we compute for the 66/66 2+2 cycloaddition dimer, is 9.05 Å while in the low-dimensionality polymers it is found to be between 9.02 and 9.18 Å [5,6]. Also, for the recent graphullerene [12,13], the computed dimer distances are 9.23 and 9.09 Å while the experimental bonding distance are 9.23 and 9.16 Å respectively. Hence, relating bonding distances to bonding schemes constitutes

* Corresponding author.
** Corresponding author.
E-mail addresses: jorgelaranjeira@ua.pt (J. Laranjeira), manuelmelle@ua.pt (M. Melle-Franco).

https://doi.org/10.1016/j.carbon.2023.118209
Received 29 March 2023; Received in revised form 9 June 2023; Accepted 12 June 2023
Available online 14 June 2023

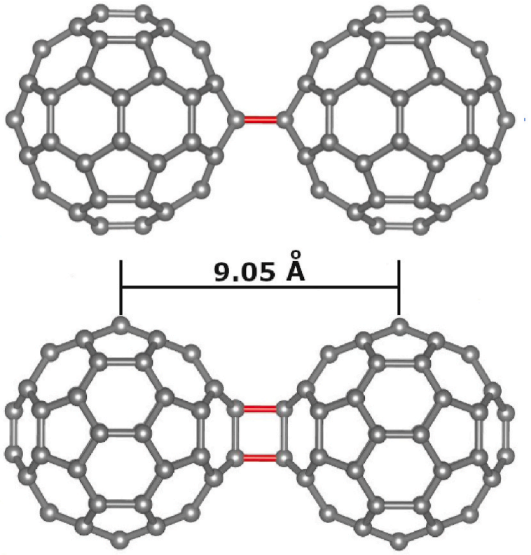

Fig. 1. The most stable and well-studied C_{60} dimer bonded via 66/66 2+2 cycloaddition, views on two orthogonal axes. Red lines highlight the intermolecular bonds, black lines show how the intermolecular distance is defined. (A colour version of this figure can be viewed online.)

a simple yet accurate interpretation tool for the C_{60} crystal structure assignment, rendering covalent C_{60} dimers specifically relevant to compute and understand.

In the 90s and beginning of the 2000s, several studies regarding dimers were presented, nevertheless, to the best of our knowledge, no more than 12 dimers have been described altogether. Here, we consider, unless noted, C_{60} covalent dimers, that is dimers where the forming fullerene molecules are joined by intermolecular bonds. Strout et al. [4] performed probably the most extensive C_{60} dimerization study which addressed the 2+2 cycloadditions and a 2+4 cycloaddition. This last bonding scheme, following our notation, corresponds to a double 6/56 4+2 cycloaddition, since two 2+4 cycloaddition reactions, involving one hexagon (6) and one intramolecular single bond (56) each, are present.

Later, in 1994, Adams et al. [14] proposed three other bonding schemes, two bonding the molecules via their hexagons and one between their pentagons. In the bonding between hexagons, the six atoms from one hexagon bond to the six atoms of the other hexagon, which can be obtained in the following two ways: 1) the hexagons of the two molecules align with each other (as well as the pentagons); 2) the hexagons from one molecule align with the pentagons of the other. When possible, we will keep the cycloaddition notation for the formed dimers nomenclature thus, in this case the dimers will be named, for instance, “triple 66/66 2+2 cycloaddition” (or “triple 56/56 2+2 cycloaddition”) and “triple 56/66 2+2 cycloaddition” respectively. In the bonding between pentagons the five atoms from one pentagon bond to the five atoms of the other, the dimer will be referred to as “double 56/56 2+2 cycloaddition plus single bond”. More details about this bonding nomenclature are available in the supporting information (SI) section A. In 2007 Liu et al. [15] studied again the two dimers bonded via hexagons confirming that they are thermodynamically stable and thus, could be observed experimentally.

Osawa et al. [16] reported the two possible 6/6 4+4 cycloaddition bonded dimers, while Matsuzawa et al. [17] also considered the 6/6 4+4 cycloaddition dimers and added one of the two 66/6 2+4 cycloaddition dimers to their calculations. Besides the mentioned dimers, the single bond dimer (SB) was also considered [18]. In all of the works mentioned so far, the lowest energy dimer was consistently found to be the 66/66 2+2 cycloaddition [4,14,15,18].

Apart from dimers formed just with pristine, i.e. unfunctionalized, C_{60}, there have also been numerous studies of dimers formed with other intermediates as well as coalescence products [4,19,20]. In addition, there have been studies on the dimerization and coalescence of C_{60} inside carbon nanotubes [5,21,22]. Note that although some of these systems also did appear in our calculations, for simplicity, they were not considered in our analysis and will not be discussed. Nevertheless, coalescence products might improve the understanding of amorphous carbon phase formation from C_{60} [23] or other phases where the C_{60} cage is broken [24] and might be the object of future studies.

The new systems reported here have been obtained fundamentally with AutoMeKin [25–27], an automatic computational procedure to find and characterize chemical reaction paths, and extended by manual construction following geometric considerations. We report a total of 41 stable dimers computed at DFT level. From these, 25 were obtained with AutoMeKin, the others were built from geometric considerations or obtained from the literature. The molecular structure and relative stability of all dimers were computed at the TPSS-Def2-TZVPP/B3LYP-6-31G(d,p) theory level augmented by D3 dispersion with Becke–Johnson damping. All the dimers studied present C_{60} distances between 8.04 Å and 9.23 Å which renders some of these bridging patterns suitable candidates to be present in 3D C_{60} polymers.

2. Methods

First, we performed a benchmark calculation of the dimer bonding energies for four different Hamiltonians, namely: TPSS-Def2-TZVPP-D3BJ/TPSS-6-31G(d,p)- D3BJ, TPSS-Def2-TZVPP-D3BJ/B3LYP-6-31G(d,p)-D3BJ, TPSS-6-31G(d,p)-D3BJ and B3LYP-6-31G(d,p)-D3BJ, on the lowest five energy C_{60} dimers, Table 1. The TPSS-Def2-TZVPP-D3BJ Hamiltonian was chosen after a recent benchmark study comparing the C_{60} isomerization energies with 115 methodologies which recommended this method based on its accuracy [28]. The bonding energy was computed by subtracting the energy of two isolated C_{60} to the energy of each dimer: $\Delta E_{Bond} = E_{dimer} - 2E_{C_{60}}$.

The Basis Set Superposition Error (BSSE) was evaluated in a non-covalent dimer, and found to be sizable, around 0.1 eV, for bonding energies with the smaller, DZP, basis sets, Table 1. After the BSSE correction, both levels of theory yielded values differing less than 5 meV. Interestingly, relative energies were very similar, and also similar results were found for all DFT functionals. Considering this, we selected the TPSS-Def2-TZVPP-D3BJ/B3LYP-6-31G(d,p)-D3BJ methodology as it yields a good compromise between accuracy and computational cost. Namely, we performed the geometry optimizations at the B3LYP-6-31G(d,p) [29,30] level augmented by the D3 van der Waals correction [31,32] with Becke–Johnson damping [33] (B3LYP-6-31G(d,p)-D3BJ) followed by a single point calculation with TPSS-Def2- TZVPP Hamiltonian [34,35] also augmented by the D3 van der Waals correction with Becke–Johnson damping (TPSS-Def2-TZVPP-D3BJ) for the energies. Hessian calculations were performed in all presented geometries at the B3LYP-6-31G(d,p)-D3BJ level to explicitly check the absence of negative frequencies. Cartesian coordinates of the optimized geometries of all dimers are available in section F of the SI. All calculations were performed with Gaussian09 [36].

We explicitly analyzed the dispersion contribution to the bonding energy, as this contribution is missing in most early DFT and semi-empirical studies. The dispersion correction shifts bonding energies to more binding values, for the B3LYP-6-31G(d,p) functional the maximum shift is 1.34 eV and the average one is 0.78 eV. For the TPSS-Def2-TZVPP functional the stabilization is lower, the maximum shift is 1.15 eV and the average 0.68 eV. This indicates that there is a consistent attractive dispersion contribution to the bonding interaction in all covalently bonded C_{60} dimers. In fact, without van der Waals correction, all dimers are metastable compared to the isolated C_{60} molecule, see SI, Table S1 and figures S1 and S2.

The InfraRed (IR) spectra of all dimers were also computed and are available in section E of the SI. The comparative analysis of all the

Table 1
Bonding energies of the five lowest energy C_{60}+C_{60} dimers and a non-covalent C_{60}+C_{60} dimer computed at different levels of theory with and without the Basis Set Superposition Error (BSSE) correction. All values in eV.

Theory level	Dimer 1	Dimer 2	Dimer 3	Dimer 4	Dimer 5	Non-Covalent Dimer	Non-Covalent Dimer BSSE corrected
B3LYP-6-31G(d,p)-D3BJ	−0.654	0.206	0.584	1.057	1.093	−0.457	−0.351
TPSS-6-31G(d,p)-D3BJ	−0.542	0.213	0.530	0.964	0.990	–	–
TPSS-Def2-TZVPP-D3BJ/TPSS-6-31G(d,p)-D3BJ	−0.251	0.493	0.740	1.243	1.268	–	–
TPSS-Def2-TZVPP-D3BJ/B3LYP-6-31G(d,p)-D3BJ	−0.249	0.499	0.744	1.250	1.277	−0.360	−0.346

spectra reveals that the active frequencies of the C_{60} molecule are still present in each C_{60} dimer yet with different relative intensities. In addition, there are new peaks due to the symmetry reduction imposed by the new intermolecular bonds.

To systematically explore possible C_{60} dimer minima we employed AutoMeKin (AMK) [25–27], a software designed to find reaction mechanisms. AMK analyzes high-energy molecular dynamics trajectories via graph theory to search for structural transformations. When a structural transformation, such as bonds breaking or forming, is detected it finds and characterizes the transition state via its second-order derivatives. From the transition state, the intrinsic reaction coordinate (IRC) method is then used to obtain reactants and products. For this, 2.25 ns were run altogether via 4500, 500 fs long, independent molecular dynamics of two C_{60} molecules in a high energy bonding configuration. The dynamics were run with a specially modified version of MOPAC2016 [37] using the PM7 [38] Hamiltonian with a time step of 0.5 fs and temperatures between 6000 K and 10000 K. The simulations led to the discovery of 9622 structures, but only a subset of them were identified as C_{60} dimers. The remaining structures were either molecular fragments or other fullerene configurations with higher energy levels. After the complete procedure, AMK yielded 64 unique minima at the PM7 level, which upon refinement with DFT were reduced to 25 different minima. Note that AMK so far has been used in molecules $\leq$30 atoms [39], so this study, on a system with 120 atoms, showcases how the AMK methodology can be successfully extended to other problems.

In addition, for completeness, we have comprehensively searched for reported dimers in literature and also constructed other bonding schemes considering the geometric possibilities allowed by the molecule. The following labels reveal the procedure followed for each minimum: L, literature, G, geometric considerations and AMK, Table S3. To build dimers from geometric considerations, we went through the possibilities of bonding between each molecular element of geometry avoiding large deformations. Three geometry elements: chemical bonds, pentagons, or hexagons were considered with a maximum of two of these elements being combined at a time. For instance, the two "5/6 3+3″ bonds may be constructed taking into consideration the bridging of one pentagon to one hexagon while the "double 66/66 4+4" takes into consideration the bridging of two hexagons from each molecule. For simplicity, we only considered systems with an even number of intermolecular bonds in this procedure.

We present the HOMO-LUMO gaps at the B3LYP- 6-31G(d,p) level as this Hamiltonian is expected to yield closer values to experiment [40]. Note that all calculations were first run without spin polarization, and, in the cases where structures were found to be unstable under these conditions, they were then run considering triplet or quintuplet ground states. This procedure yielded 12 dimers with spin-polarized ground states. In all cases, no initial symmetry constraints were used in the geometry optimizations.

3. Results and discussion

The dimer structures found are comprehensively summarized in Table 2 by increasing energy with their symmetry, number of intermolecular bonds, HOMO-LUMO gap, bonding energy and the distance between C_{60} molecules. A graphical rendering for all the bonding schemes found on these dimers together with some others that were found by AMK but are not stable at the DFT level, can be found on the SI, Table S3. Relevantly, of the 12 dimers previously reported just the 6/66 2+4 cycloaddition reported by Matsuzawa et al. [17] was found not to be stable in our study, although it was found by AMK (AMK minimum 3097) indicating that at the semiempirical PM7 level, this dimer is stable.

Only one covalent dimer with a bonding energy of −0.25 eV was found to be thermodynamically more stable, i.e. exothermic, than the isolated C_{60} molecules. In comparison, the least stable dimer is considerably more endothermic with a bonding energy of 7.95 eV. As a reference, we also computed the energy of the non-covalent dimer, −0.36 eV, which is more stable than the isolated molecule and any covalent dimer. These results match experimental observations since the only, experimentally observed, covalent dimer is fruit of the 66/66 2+2 cycloaddition [2–4] and at ambient conditions, C_{60} molecules are not covalently bound in the solid state. More exotic bonding configurations, for instance, corresponding to the 56/56 2+2 cycloaddition [8], can be found in three-dimensional crystals formed under high-pressure treatments, where the 66/66 2+2 cycloaddition bonding scheme alone cannot be used to bond all molecules in a three-dimensional extended system.

Relevantly, with more extreme pressures, higher energy minima can be reached with reduced C_{60} distances, fitting the trend shown in Fig. 2 a) where the distances between molecules show a monotonous decrease with increasing bonding energies. Furthermore, several of our dimers have shorter distances than reported coalescence products, see for instance the report by Strout et al. [4]. This indicates, that very short distances, below 8.3 Å, may alternatively be explained by C_{60} molecules bonded by the patterns reported here. Also, it is important to notice that although all the bonding schemes yield lower HOMO-LUMO gaps compared to C_{60}, no clear trend between this quantity and energy, number of bonds or intermolecular distance was found.

Interestingly, some of the found dimers are minima only with spin-polarized, triplet or quintuplet, wave-functions. If the minimization is performed without spin-polarization, the dimers either break into C_{60} molecules or transform into the more stable 66/66 2+2 cycloaddition dimer. Dimers with spin-polarized ground states, in Table 2, are marked with a star (*) in the HOMO-LUMO value. In addition, the value reported corresponds to the average gap for α and β electrons, Table S2. C_{60} dimer minima 3, 8, 10, 27 and 37 have triplet ground states while minima 16, 17, 21, 22, 24, 25 and 32 have quintuplet ground states. This sheds light on the potential importance of spin-polarization in high-pressure polymerized C_{60} since some of these bonds may be present in high-pressure formed structures and thus, models built with them probably require spin-polarized Hamiltonians to be properly accounted for. In fact, Bernasconi et al. [42] took this into consideration while computing three-dimensional C_{60} polymers noticing that some of the modeled structures had more stable spin-polarized ground states.

After the dimer formation, all the C_{60} molecules present some degree of deformation with respect to their original structure. To quantify the degree of molecular deformation we computed the asphericity of each molecule defined as the largest absolute value obtained subtracting the distance to each fullerene center of mass for each atom in the dimer to the pristine C_{60} radius, 3.51 Å. Asphericity values are summarized in Table S2, relevantly, the dimers with higher symmetries than C_s have the same degree of deformation in both molecules, i.e. the same sphericity.

Table 2
Energetics and distances of C_{60}+C_{60} dimers computed at TPSS-Def2-TZVPP-D3BJ/B3LYP-6-31G(d,p)-D3BJ level. The HOMO-LUMO gaps presented were computed with B3LYP-6-31G(d,p)-D3BJ with * indicating that the presented value is an average of the α and β spin channels gaps. The molecular distance given in the last column corresponds to the distances between the C_{60} molecular centers of mass. Dimers referred to as AMK# could not be described by the naming scheme and correspond to an internal sequential reference produced by AMK during the generation.

Dimer	Dimer denomination	Sym.	Interm. bonds	HOMO-LUMO gap (eV)	ΔE_{Bond} (eV)	Mol. dist. Å
	C_{60}	I_h	0	2.85	–	–
	Non covalent	C_1	0	2.60	−0.360	9.88
1	66/66 2+2	D_{2h}	2	2.51	−0.249	9.05
2	56/66 2+2	C_s	2	1.82	0.499	9.07
3	SB	C_{2h}	1	1.91*	0.744	9.23
4	56/65 2+2	C_{2h}	2	1.70	1.250	9.09
5	56/56 2+2	C_{2v}	2	1.75	1.277	9.10
6	double 66/66 2+2	C_{2v}	4	2.49	1.468	8.64
7	double 56/66 2+2 M2	C_s	4	2.46	1.837	8.65
8	5/66 3+2	C_s	2	1.88*	2.163	8.91
9	double 56/56 2+2	C_{2v}	4	2.34	2.253	8.66
10	AMK5678	C_1	3	1.56*	2.336	8.85
11	6/66 3+2	C_1	2	0.75	2.387	8.87
12	6/6 4+4 M1	C_{2v}	2	1.98	2.622	8.81
13	triple 66/65 2+2	D_{3d}	6	2.39	2.642	8.44
14	6/6 4+4 M2	C_{2h}	2	1.80	2.644	8.81
15	triple 66/66 2+2	D_{3h}	6	2.43	2.678	8.44
16	6/6 3+4 M2	C_1	2	1.89*	2.892	8.80
17	6/6 3+3 M3	C_2	2	1.86*	3.139	8.77
18	double 56/66 2+2 M1	C_s	4	1.57	3.255	8.69
19	5/6 3+4 M2	C_s	2	1.01	3.310	8.87
20	5/6 3+4 M1	C_s	2	1.02	3.333	8.87
21	6/56 3+2 M2	C_1	2	1.64*	3.380	8.87
22	6/56 3+2 M1	C_1	2	1.62*	3.420	8.87
23	double 56/65 2+2	C_s	4	1.52	3.653	8.71
24	5/5 3+3 M1	C_{2h}	2	1.65*	3.676	8.89
25	6/6 3+4 M1	C_1	2	1.39*	3.914	8.77
26	double 56/56 2+2	C_{2v}	4	1.23	4.495	8.75
27	AMK6163	C_1	3	1.83*	4.626	8.41
28	double 56/56 2+2 plus SB	D_{5h}	5	0.74	4.829	8.68
29	double 6/56 4+2	C_{2h}	4	2.34	5.025	8.62
30	5/56 3+2 plus 6/56 4+2	C_s	4	1.53	5.117	8.67
31	double 5/5 2+3	C_{2h}	4	1.11	5.263	8.72
32	5/6 3+3 plus 56/6 2+3	C_1	4	1.42*	5.535	8.62
33	AMK7077	C_s	4	0.88	6.316	8.29
34	AMK6511	C_1	4	1.68	6.434	8.28
35	AMK7610	C_s	4	0.95	6.717	8.25
36	5/5 3+3 plus 6/6 4+4	C_{2v}	4	0.77	6.845	8.05
37	double 56/65 3+4	C_{2h}	4	0.76*	6.909	8.10
38	5/6 3+4 plus 6/6 4+4	C_s	4	0.94	6.997	8.04
39	double 66/66 4+4	D_{2h}	4	1.64	7.026	8.05
40	AMK8161	C_s	4	2.51	7.582	8.28
41	double 66/66 4+4 plus 66/66 2+2	D_{2h}	6	2.01	7.950	8.16

In this case, asphericity values range from 0.25 Å for C_{60} dimer minima 13 and 15 to 0.75 Å for minima 37 and 39. Fig. 2 b) shows the asphericity values as a function of the bonding energy. The asphericity qualitatively increases with increasingly endothermic bonding energies, indicating how higher deformation is clearly related to higher energetics and to the more extreme conditions needed for the synthesis of structures displaying these bonding schemes. In fact, the largest asphericity is found for one of the most energetic dimers, minimum 40, with a value of 1.30 Å.

AMK was crucial in finding exotic bonding schemes, like minima 33 and 35 where one of the molecules is pinched allowing the bonding between one pentagon (for minimum 33) or hexagon (for minimum 35) of one molecule to one hexagon and one pentagon of the other molecule, see Fig. 3 a) and b). This pinching implies a high asphericity value in the pinched molecule, ~1.0 Å, while the other molecule has nearly half that value in both dimers, Table S2. In both cases, this translates to remarkably short distances, ~8.25 Å, and is illustrative for dimers with short bonding distances, ≤8.4 Å. Furthermore, AMK found another peculiar bond, the double 5/5 2+3 cycloaddition (minimum 31), that was already present in a novel clathrate structure with very similar distances to the ones presented here [11].

Buga et al. [41] presented a series of six experimental crystalline phases obtained by pressurizing C_{60} between 11.5 and 13 GPa. In their report, structures are body-centered orthorhombic with the Immm space group ($I^{\nu}_{o}D^{25}_{2h}$ in Schönflies notation) and presented their lattice parameters although no actual structure was proposed. Since their structures are body-centered orthorhombic, each of them has three distinct C_{60} distances, Table 3. In Fig. 2 a), we show a green area where these intermolecular distances lie. The longest distance found in this study is ~9.2 Å, in minimum 3. Note that as distances by different computational methods may differ, if slightly, we have considered a ±0.2 Å of length "flexibility" to our intermolecular distance values. In addition, molecules may also have additional deformations while in the crystalline phase, therefore hindering the direct correspondence between dimer distances and crystalline distances. This is observed, for instance, in the 66/66 2+2 cycloaddition dimer that shows different experimental distances lying between 9.02 and 9.18 Å [5,6]. Hence, experimental intermolecular distances larger than 9.3 Å in Table 3, may be due to either a single bond or no bond between neighboring molecules. Interestingly, several experimental distances between C_{60} molecules were found to be between 8.65 and 8.80 Å, see Table 3, which are common distances in our dimers. Considering this, it is possible that some of our bonding schemes are responsible for the distances found in these polymerized experimental phases.

In addition, there are other structures in the literature still to be resolved, like the one reported by Yamanaka et al. [9]. Although a complete crystalline structure was proposed, the structure changed considerably when optimized with DFT without constraints [42,43]. Namely, Yamanaka et al. derived experimental lattice parameters of 7.86, 8.59 and 12.73 Å and a body-centered orthorhombic structure, with corresponding distances of 7.86, 8.59 and 8.62 Å, indicated in Fig. 2 a) by the red lines. The authors assigned these distances to double 66/66 4+4, no bond and 6/6 3+3 cycloaddition, respectively. Indeed, the 6/6 3+3 cycloaddition dimer, minimum 17, and 66/66 4+4 cycloaddition dimer, minimum 39, have bonding distances in the appropriate range to explain this experimental data. Nevertheless, these bonding schemes were already used by Zipoli and Bernasconi [42] to construct crystalline structures and fail to reproduce the experimental lattice parameters. Thus, other bonding schemes must be considered. We present here several potential alternatives within the observed range of distances.

Conversely, although the comparison of the distance is a simple, yet effective tool, we would like to emphasize that bonding patterns, which are stable in dimers may not be stable or not even geometrically possible in specific crystalline structures. For instance, minimum 4, although

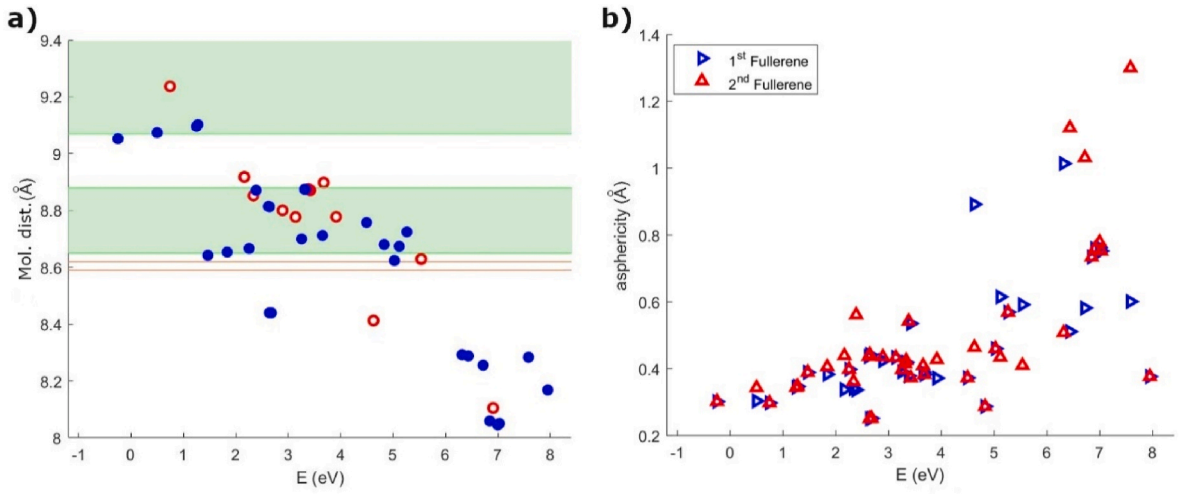

Fig. 2. a) Intermolecular distances as a function of the bonding energy computed at TPSS-Def2-TZVPP-D3BJ/B3LYP-6-31G(d,p)-D3BJ level of theory. Red hollow circles indicate open-shell ground states while blue full circles represent closed-shell ground states. Red lines and green regions correspond to the experimental molecular distances reported by Yamanaka et al. [9] and Buga et al. [41] respectively. b) Asphericity as a function of the bonding energy for the first C_{60} molecule (blue) and the second C_{60} molecule (red) forming each dimer. (A colour version of this figure can be viewed online.)

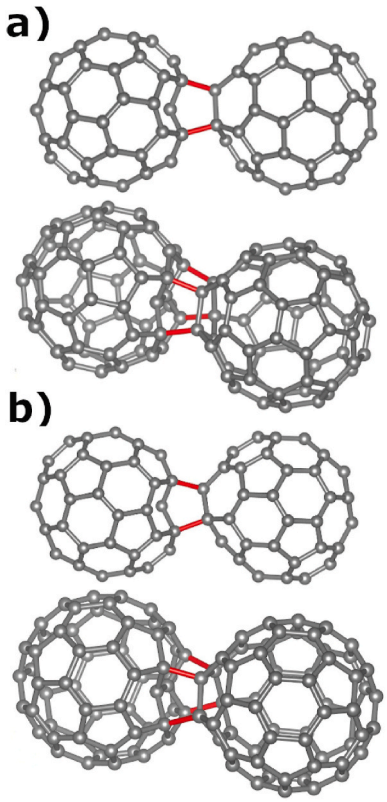

Fig. 3. Two exotic bonding patterns obtained with AMK, two views. a) Dimer AMK7077, minimum 33, where the two molecules are bonded between the pentagon of the right molecule and one hexagon plus one pentagon of the left molecule. b) Dimer AMK7610, minimum 35 where the two molecules are bonded between the hexagon of the right molecule and one hexagon plus one pentagon of the left molecule. (A colour version of this figure can be viewed online.)

geometrically capable to bond to all the neighboring molecules in a crystalline fcc structure, turns out to be unstable in such configuration [7,8]. On the other hand, the same minimum is present in other reported structures, such as in a 3D-rhombohedral phase [10] and in the recent graphullerene [13], proving that the molecular environment as a whole has to be considered to evaluate the existence of these patterns.

Table 3
Polymerized C_{60} intermolecular distances inferred from the high-pressure experimental lattice parameters and overall symmetry reported by Buga et al. [41], see text for details.

Sample Nº	1	2	3	4	5	6
distance 1 (Å)	9.07	8.73	8.69	8.68	8.67	8.65
distance 2 (Å)	9.47	9.16	8.88	8.84	8.81	8.78
distance 3 (Å)	9.19	9.05	8.88	8.85	8.83	8.79

4. Conclusion

A comprehensive exploration and in-depth characterization of a large number of C_{60} dimers built from high energy molecular dynamics trajectories through the AMK methodology was performed. Several new C_{60} bonding schemes potentially relevant to understand polymeric phases were found and were energetically, structurally and electronically classified, increasing the number of known C_{60} dimers from 12 to 41. Some of the new dimers have bonding schemes matching experimental intermolecular distances observed on high-pressure high-temperature polymerized C_{60} yet to be understood, for instance in the works of Buga et al. or Yamanaka et al. [9,41]. Relevantly, 12 of these dimers, i.e. 29 %, have spin-polarized ground states, which emphasizes that spin-polarization should be explicitly taken into consideration to properly model crystalline structures, especially with metallic or electronic exotic properties. This work paves the way for the exploration of novel extended 1D, 2D and 3D structures based on the bonding schemes presented here obtainable by HPHT treatment or more recent alternative routes [12,13].

CRediT authorship contribution statement

Jorge Laranjeira: Conceptualization, Methodology, Formal analysis, Investigation, Data curation, Writing – original draft, Writing – review & editing, Visualization, Funding acquisition. **Karol Strutyński:** Writing – review & editing. **Leonel Marques:** Writing – review & editing. **Emilio Martínez-Núñez:** Methodology, Formal analysis, Software, Validation, Funding acquisition. **Manuel Melle-Franco:** Conceptualization, Methodology, Software, Resources, Writing – review & editing,

Supervision, Funding acquisition, All authors have read and agreed to the published version of the manuscript.

Declaration of competing interest

The authors declare that they have no known competing financial interests or personal relationships that could have appeared to influence the work reported in this paper

Acknowledgements

This work was developed within the scope of the project CICECO-Aveiro Institute of Materials, UIDB/50011/2020, UIDP/50011/2020 & LA/P/0006/2020, financed by national funds through the FCT/MCTES (PIDDAC) and 2022.07534.CEECIND and IF/00894/2015 contracts funded by FCT. J. Laranjeira acknowledges a PhD grant from FCT (SFRH/BD/139327/2018).

This work was partially supported by the Consellería de Cultura, Educacíon e Ordenacíon Universitaria (Grupo de referencia competitiva ED431C 2021/40), and the Ministerio de Ciencia e Innovacíon through Grant #PID2019-107307RB-I00.

The work has been performed under the project HPC-EUROPA3 (INFRAIA-2016-1-730897), with the support of the EC Research Innovation Action under the H2020 Programme; in particular, the author gratefully acknowledges the support of the computer resources and technical support provided by BSC.

Appendix A. Supplementary data

Supplementary data to this article can be found online at https://doi.org/10.1016/j.carbon.2023.118209.

References

[1] A. Harris, R. Sachidanandam, Orientational ordering of icosahedra in solid C_{60}, Phys. Rev. B 46 (1992) 4944–4957, https://doi.org/10.1103/PhysRevB.46.4944.
[2] A. Rao, P. Zhou, K.-A. Wang, G. Hager, J. Holden, Y. Wang, W.-T. Lee, X.-X. Bi, P. Eklund, D. Cornett, M. Duncan, I. Amster, Photoinduced polymerization of solid C_{60} films, Science 259 (1993) 955–957, https://doi.org/10.1126/science.259.5097.955.
[3] V. Davydov, L. Kashevarova, A. Rakhmanina, V. Senyavin, O. Pronina, N. Oleynikov, V. Agafonov, R. Ceolin, H. Allouchi, H. Szwarc, Pressure-induced dimerization of fullerene C_{60}: a kinetic study, Chem. Phys. Lett. 333 (2001) 224–229, https://doi.org/10.1016/S0009-2614(00)01379-8.
[4] D. Strout, R. Murry, C. Xu, W. Eckhoff, G. Odom, G. Scuseria, A theoretical study of buckminsterfullerene reaction products: C_{60}+C_{60}, Chem. Phys. Lett. 214 (1993) 576–582, https://doi.org/10.1016/0009-2614(93)85686-I.
[5] M. Álvarez−Murga, J.L. Hodeau, Structural phase transitions of C_{60} under high-pressure and high-temperature, Carbon 82 (2015) 381–407, https://doi.org/10.1016/j.carbon.2014.10.083.
[6] M. Núñez−Regueiro, L. Marques, J.L. Hodeau, O. Bethoux, M. Perroux, Polymerized fullerite structures, Phys. Rev. Lett. 74 (1995) 278–281, https://doi.org/10.1103/PhysRevLett.74.278.
[7] J. Laranjeira, L. Marques, M. Mezouar, M. Melle-Franco, K. Strutynski, Bonding frustration in the 9.5 GPa fcc polymeric C_{60}, Phys. Stat. Sol. – RRL 11 (2017), 1700343, https://doi.org/10.1002/pssr.201700343.
[8] J. Laranjeira, L. Marques, N. Fortunato, M. Melle-Franco, K. Strutynski, M. Barroso, Three-dimensional C_{60} polymers with ordered binary-alloy-type structures, Carbon 137 (2018) 511–518, https://doi.org/10.1016/j.carbon.2018.05.070.
[9] S. Yamanaka, A. Kubo, K. Inumaru, K. Komaguchi, N. Kini, T. Inoue, T. Irifune, Electron conductive three-dimensional polymer of cuboidal C_{60}, Phys. Rev. Lett. 96 (2006), 076602, https://doi.org/10.1103/PhysRevLett.96.076602.
[10] S. Yamanaka, N. Kini, A. Kubo, S. Jida, H. Kuramoto, Topochemical 3D polymerization of C_{60} under high pressure at elevated temperatures, J. Am. Chem. Soc. 130 (2008) 4303–4309, https://doi.org/10.1021/ja076761k.
[11] J. Laranjeira, L. Marques, M. Melle-Franco, K. Strutynski, M. Barroso, Clathrate structure of polymerized fullerite C_{60}, Carbon 194 (2022) 297–302, https://doi.org/10.1016/j.carbon.2022.03.055.
[12] L. Hou, X. Cui, B. Guan, S. Wang, R. Li, Y. Liu, D. Zhu, J. Zheng, Synthesis of a monolayer fullerene network, Nature 606 (2022) 507–510, https://doi.org/10.1038/s41586-022-04771-5.
[13] E. Meirzadeh, A. Evans, M. Rezaee, M. Milich, C. Dionne, T. Darlington, S.T. Bao, A. Bartholomew, T. Handa, D. Rizzo, R. Wiscons, M. Reza, A. Zangiabadi, N. Fardian-Melamed, A. Crowther, J. Schuck, D. Basov, X. Zhu, A. Giri, P. Hopkins, P. Kim, M. Steigerwald, J. Yang, C. Nuckolls, X. Roy, A few-layer covalent network of fullerenes, Nature 613 (2023) 71–76, https://doi.org/10.1038/s41586-022-05401-w.
[14] G. Adams, J. Page, O. Sankey, M. O'Keeffe, Polymerized C_{60} studied by first-principles molecular dynamics, Phys. Rev. B 50 (1994) 17471–17479, https://doi.org/10.1103/PhysRevB.50.17471.
[15] F.-L. Liu, X.-X. Zhao, Two intact C_{60} cages linked by six carbon–carbon single bonds, J. Mol. Struct.: THEOCHEM 804 (2007) 117–121, https://doi.org/10.1016/j.theochem.2006.10.018.
[16] S. Ōsawa, E. Ōsawa, Y. Hirose, Doubly bonded C_{60} dimers and congeners: computational studies of structures, bond energies and transformations, Fullerene Sci. Technol. 3 (1995) 565–585, https://doi.org/10.1080/153638X9508543808.
[17] N. Matsuzawa, M. Ata, D. Dixon, G. Fitzgerald, Dimerization of C_{60}: the formation of dumbbell-shaped C_{120}, J. Phys. Chem. 98 (10) (1994) 2555–2563, https://doi.org/10.1021/j100061a009.
[18] G. Scuseria, What is the lowest-energy isomer of the C_{60} dimer? Chem. Phys. Lett. 257 (1996) 583–586, https://doi.org/10.1016/0009-2614(96)00599-4.
[19] P. Fowler, D. Mitchell, R. Taylor, G. Seifert, Structures and energetics of dimeric fullerene and fullerene oxide derivatives, J. Chem. Soc., Perkin Trans. 2 (1997) 1901–1905, https://doi.org/10.1039/A703836D.
[20] M. Diudea, C. Nagy, O. Ursu, T. Balaban, C_{60} dimers revisited, Fullerenes, Nanotub. Carbon Nanostruct. 11 (2003) 245–255, https://doi.org/10.1081/FST-120024043.
[21] M. Koshino, Y. Niimi, E. Nakamura, H. Kataura, T. Okazaki, K. Suenaga, S. Iijima, Analysis of the reactivity and selectivity of fullerene dimerization reactions at the atomic level, Nat. Chem. 2 (2010) 117–124, https://doi.org/10.1038/nchem.482.
[22] T. Shimizu, D. Lungerich, K. Harano, E. Nakamura, Time-resolved imaging of stochastic cascade reactions over a submillisecond to second time range at the angstrom level, J. Am. Chem. Soc. 144 (2022) 9797–9805, https://doi.org/10.1021/jacs.2c02297.
[23] S. Zhang, Z. Li, K. Luo, J. He, Y. Gao, A. Soldatov, V. Benavides, K. Shi, A. Nie, B. Zhang, W. Hu, M. Ma, Y. Liu, B. Wen, G. Gao, B. Liu, Y. Zhang, Y. Shu, D. Yu, X.-F. Zhou, Z. Zhao, B. Xu, L. Su, G. Yang, O. Chernogorova, Y. Tian, Discovery of carbon-based strongest and hardest amorphous material, Natl. Sci. Rev. 9 (1) (2021), https://doi.org/10.1093/nsr/nwab140 nwab140.
[24] F. Pan, K. Ni, T. Xu, H. Chen, Y. Wang, K. Gong, C. Liu, X. Li, M.-L. Lin, S. Li, X. Wang, W. Yan, W. Yin, P.-H. Tan, L. Sun, D. Yu, R. Ruoff, Y. Zhu, Long-range ordered porous carbons produced from C_{60}, Nature 614 (2023) 95–101, https://doi.org/10.1038/s41586-022-05532-0.
[25] E. Martínez-Núñez, An automated method to find transition states using chemical dynamics simulations, J. Comput. Chem. 36 (2015) 222–234, https://doi.org/10.1002/jcc.23790.
[26] E. Martínez-Núñez, An automated transition state search using classical trajectories initialized at multiple minima, Phys. Chem. Chem. Phys. 17 (2015) 14912–14921, https://doi.org/10.1039/C5CP02175H.
[27] A. Rodriguez, R. Rodriguez-Fernandez, S. Vazquez, G. Barnes, J. Stewart, E. Martínez-Núñez, tsscds2018: a code for automated discovery of chemical reaction mechanisms and solving the kinetics, J. Comput. Chem. 39 (2018) 1922–1930, https://doi.org/10.1002/jcc.25370.
[28] A. Karton, S. Waite, A. Page, Performance of DFT for C_{60} isomerization energies: a noticeable exception to jacob's ladder, J. Phys. Chem. A 123 (2019) 257–266, https://doi.org/10.1021/acs.jpca.8b10240.
[29] A. Becke, A new mixing of Hartree–Fock and local density-functional theories, J. Chem. Phys. 98 (1993) 1372–1377, https://doi.org/10.1063/1.464304.
[30] C. Lee, W. Yang, R. Parr, Development of the colle-salvetti correlation-energy formula into a functional of the electron density, Phys. Rev. B 37 (1988) 785–789, https://doi.org/10.1103/PhysRevB.37.785.
[31] S. Grimme, J. Antony, S. Ehrlich, H. Krieg, A consistent and accurate ab initio parametrization of density functional dispersion correction (DFT-D) for the 94 elements H-Pu, J. Chem. Phys. 132 (2010), 154104, https://doi.org/10.1063/1.3382344.
[32] S. Grimme, S. Ehrlich, L. Goerigk, Effect of the damping function in dispersion corrected density functional theory, J. Comput. Chem. 32 (2011) 1456–1465, https://doi.org/10.1002/jcc.21759.
[33] A. Becke, E. Johnson, A density-functional model of the dispersion interaction, J. Chem. Phys. 123 (2005), 154101, https://doi.org/10.1063/1.2065267.
[34] J. Tao, J. Perdew, V. Staroverov, G. Scuseria, Climbing the density functional ladder: nonempirical meta–generalized gradient approximation designed for molecules and solids, Phys. Rev. Lett. 91 (2003), 146401, https://doi.org/10.1103/PhysRevLett.91.146401.
[35] F. Weigend, R. Ahlrichs, Balanced basis sets of split valence, triple zeta valence and quadruple zeta valence quality for H to Rn: design and assessment of accuracy, Phys. Chem. Chem. Phys. 7 (2005) 3297–3305, https://doi.org/10.1039/B508541A.
[36] M. Frisch, et al., Gaussian 09, Revision A.02, 2016, Gaussian Inc, Wallingford CT, 2016. http://gaussian.com/.
[37] J. Stewart, Computational Chemistry, Colorado springs, co, 2016. http://openmopac.net. (Accessed 31 January 2023) [accessed on.
[38] J. Stewart, Optimization of parameters for semiempirical methods vi: more modifications to the NDDO approximations and re-optimization of parameters, J. Mol. Model. 19 (2013) 1–32, https://doi.org/10.1007/s00894-012-1667-x.
[39] R. Jara-Toro, G. Pino, D. Glowacki, R. Shannon, E. Martínez-Núñez, Enhancing automated reaction discovery with boxed molecular dynamics in energy space, ChemSystemsChem 2 (2020), e1900024, https://doi.org/10.1002/syst.201900024.
[40] K. Sohlberg, M. Foster, What's the gap? a possible strategy for advancing theory, and an appeal for experimental structure data to drive that advance, RSC Adv. 10 (2020) 36887–36896, https://doi.org/10.1039/D0RA07496A.

[41] S. Buga, V. Blank, N. Serebryanaya, A. Dzwilewski, T. Makarova, B. Sundqvist, Electrical properties of 3D-polymeric crystalline and disordered C_{60} and C_{70} fullerites, Diam. Relat. Mater. 14 (2005) 896–901, https://doi.org/10.1016/j.diamond.2005.01.018.

[42] F. Zipoli, M. Bernasconi, First principles study of three-dimensional polymers of C_{60}: structure, electronic properties, and Raman spectra, Phys. Rev. B 77 (2008), 115432, https://doi.org/10.1103/PhysRevB.77.115432.

[43] J. Yang, J. Tse, T. Iitaka, First-principles investigation on the geometry and electronic structure of the three-dimensional cuboidal C_{60} polymer, J. Chem. Phys. 127 (2007), 134906, https://doi.org/10.1063/1.2771162.